2.5 Applications of Nuclear Techniques

2.5.1 Irradiation of eye melanoma with protons

J. de Boer, B. Lachenmayr[a], R. Birnstock, L. Rohrer, H. Steffens
[a] Augenklinik der LMU

The depth-dose curve for irradiation of eye tumors with protons follows much more closely an ideal curve than any curve obtained for radioactive sources (see fig. 1). For the benefit of patients it is therefore planned to install a treatment facility at our accelerator. For tumors located in such a position that they can be reached without traversing the eye, the proton energy of the tandem accelerator alone is sufficient. If, however, the backside of the eye must be reached the required proton energy of 55 MeV can only be attained using the post-accelerator TRITRON that is presently nearing completion. Designing the facility for Garching profits greatly from the know-how at the OPTIS facility at the Paul-Scherrer Institut (PSI) in Villigen, Switzerland, and we thank Drs. Egger, Markovits and Zografos for their help.

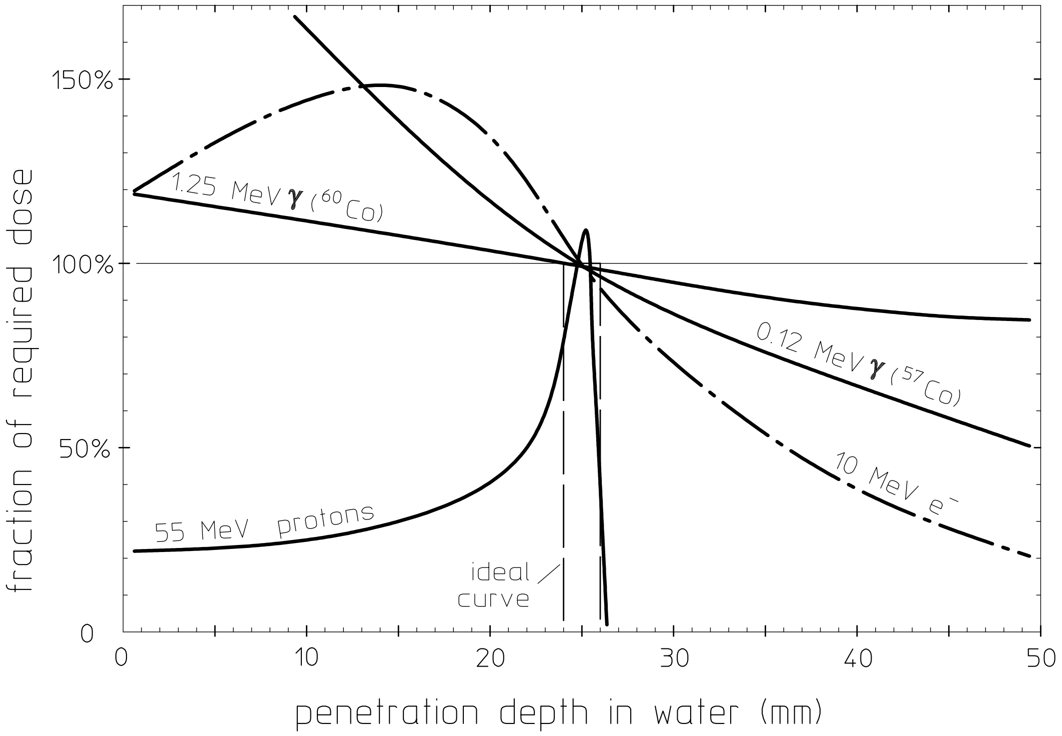

Fig. 1: Depth-dose curves for various sources of radiation compared to an ideal curve for a 2 mm thick tumor lying at a depth of 24 mm from the surface of the eye. The curves are normalized to pass through 100% at a depth of 25 mm.

2.5.2 High resolution depth profiling with the Q3D magnetic spectrograph

G. Dollinger, T. Faestermann, A. Bergmaier, M. Boulouednine, E. Schwabedissen, P. Maier-Komor and H.-J. Körner

Depth microscopy with swift heavy ions has recently been developed using an elastic recoil detection technique with superb depth resolution at the Munich tandem accelerator and its Q3D magnetic spectrograph [1, 2, 3, 4]. The method gives the possibility to analyze elemental and isotopic concentration profiles in thin films and foils with high accuracy. This technique was further developed with respect to energy resolution in connection with a large solid angle of detection and quantitative depth profiles. In addition some applications of the technique will be given in the following.

Improvements in energy resolution

60 MeV ^{58}Ni and ^{127}I ions were used as projectiles in contrast to the previous experiments, where 120 MeV Au ions were utilized [3], in order to reduce irradiation damage effects [5, 6]. The ions hit the samples to be investigated at angles between 3.5^o to 10^o relative to the surface while the scattering angle was always 15^o. The recoiled ions were detected with the Munich Q3D magnetic spectrograph, which allows in principle an energy resolution of $2{\cdot}10^{-4}$ at full solid angle. We have observed an energy resolution of $4{\cdot}10^{-4}$ with a ^{212}Po α-source (E = 8.8 MeV) using a 1 m long ionization chamber with two integrated position sensitive proportional counters as focal plane detector [7]. This high energy resolution can be obtained with 12 msr solid angle of detection. Large detection angles are required when high depth resolution of small elemental amounts is desired, otherwise the original depth profile is destroyed by irradiation damage before it is measured [3]. But the strong kinematic energy shift $\Delta E(\varphi)$ with scattering angle φ usually limits the solid angle of detection when high energy resolution is required. With the multipole element of the Q3D, however, which is an ion optical element designed for this purpose [8] we can correct for the kinematic shift up to the third order [2, 4]. The focal plane position of carbon atoms recoiled out of a thin carbon foil becomes independent of the scattering angle, when appropriatly corrected for these kinematic shifts (see cluster of pixels around energy shift zero in fig. 1a). But the accepted angle perpendicular to the bending plane of the Q3D magnets had to be reduced to $\pm 1.3^o$ because the kinematic shift in that direction which is only of second and higher orders, cannot be corrected for with the multipole element. This limitation reduces the acceptance of the Q3D to 5 msr. Another problem arises in the decreasing depth resolution with increasing depth using ERD for depth profiling. In particular a geometrical energy broadening reduces depth resolution with increasing depth beside the non-correctable effects of small angle scattering and energy loss scattering [9, 13] when large detector angles are used. This geometrical effect arises due to path length differences of the sample atoms recoiled from the same depth under different angles. These path length differences lead to energies differences which increase linearly with depth. The ion optical performance of the Q3D, however, gives also the possibility to correct for this effect as soon as a hexapole field for the correction of the second order kinematic shift is introduced. When the adjustments of the multipole fields are done at a certain energy (here designated as energy shift zero) a rotation of the angle-energy dependency is obtained at different energies. This rotation can be measured again with a thin carbon foil in transmission geometry, where the path length differences are negligible, by varying all magnetic fields by the same relative amount. That is shown for five different variations in the same picture in fig. 1a. A rotation of the angle-energy spectra in the opposite direction is achieved when e.g. the ^{13}C profile of thin ^{13}C layers in a ^{13}C/^{12}C multilayer sample is investigated in reflection geometry (fig. 1b), where the effect from path length differences is a bit larger than the ion optical effect of the Q3D. A software correction of the

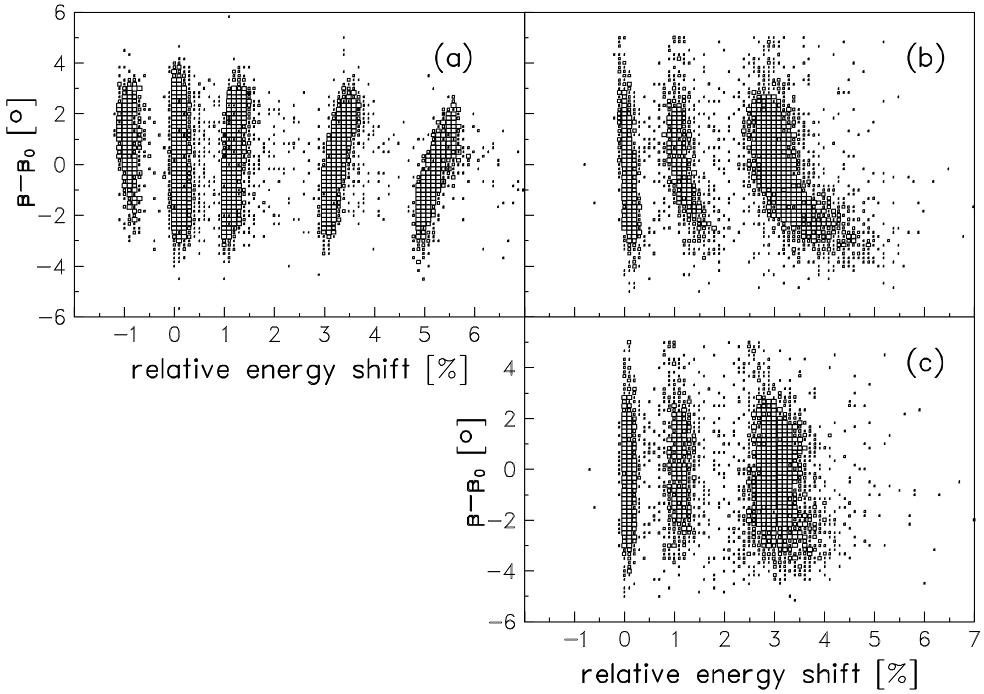

Fig. 1: Angle-energy spectra of $^{12}C^{6+}$-ions recoiled of a 2.2 μg/cm^2 thick carbon foil measdured with the focal plane gas detector in the Q3D magnetic spectrograph a) a 2.2 μg/cm^2 thick carbon foil at 5 different magnetic field settings. The kinematic shift is corrected up to the third order with the magnetic multipole element at the position designated with energy zero in this case. b) $^{13}C^{6+}$ signal of a $^{12}C/^{13}C$ multilayer system showing an opposite rotation in the angle-energy spectra as in a) due to path length dfferences of the recoiled carbon ions emerging the sample with different angles. c) Same spectra as in b) but corrected by a software routine.

remaining angle-energy dependencies can be performed without a significant loss of energy resolution as long as the gradient of the angle-energy dependence is larger than the quotient of angle resolution and intrinsic energy resolution at a certain depth.

Depth resolution

With these adjustments the depth resolution was measured at the surface of a bulk sample of highly oriented graphite. The $^{12}C^{4+}$-signal is plotted versus the carbon depth in fig. 2. It was measured with 60 MeV ^{58}Ni ions impinging at a flat angle of 3.5^o while the scattering angle was still 15^o. The spectrum rises within a relative energy loss of $7{\cdot}10^{-4}$ from 13% to 87% of the saturation value. Thus the resolution corresponds to a carbon thickness of 0.33 nm for the given geometry, ion beam and sample conditions which is equivalent to a resolution of about one interlayer spacing of the graphite (002)-layers. The same resolution could be obtained using 60 MeV ^{127}I ions incident at 5^o relative to the surface. For the heavier ions the relative energy loss, which enhances the depth resolution, is higher.

Charge distributions in ion-atom collisions and charge exchange crossections

An advantage of the elastic recoil detection (ERD) over other material analysis methods is its ability to obtain quantitative depth profiles due to the known Rutherford cross sections. In case of ERD-measurements with the Q3D magnetic spectrograph, however, the recoiled ions are separated by their momentum over charge ratio. Therefore the charge yield has to be known to convert a spectrum into a concentration profile. In order to get quantitative depth profiles for carbon isotopes, the charge yield

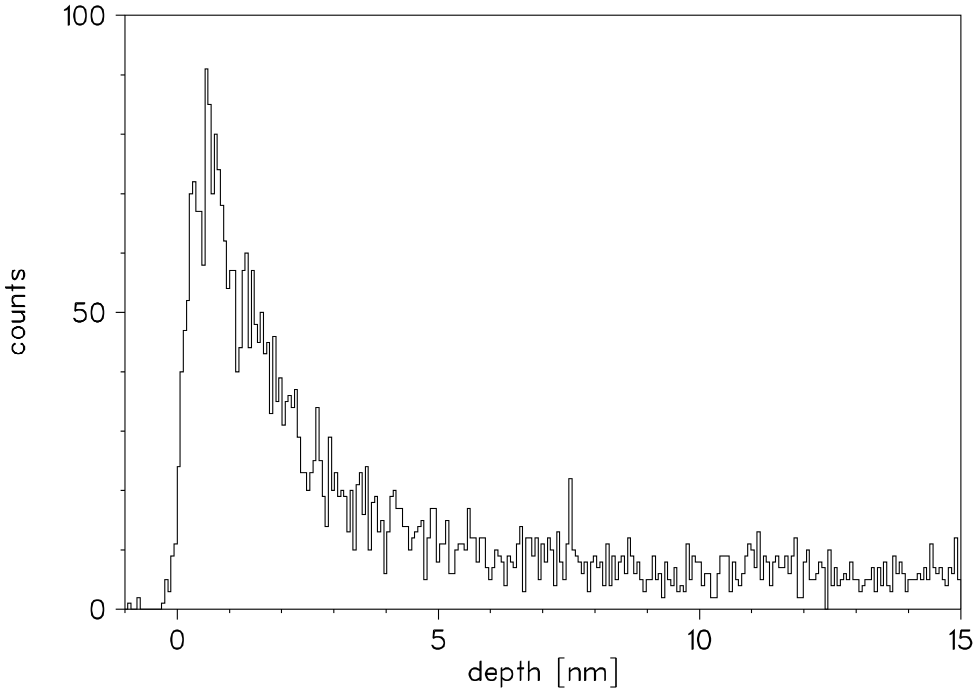

Fig. 2: $^{12}C^{4+}$ signal as an example of single layer depth resolution at the surface of higly oriented graphite obtained with 60 MeV ^{58}Ni ions. The peak near the surface arises due to charge changing collisions into the more probable higher charge states of the scattered carbon atoms. The slope at the surface shows a single carbon layer depth resolution.

as a function on energy and depth has been measured with carbon ions recoiled from highly oriented graphite. From these data the charge state distribution populated during the ion-atom collision could be extrapolated. Charge exchange cross sections and equilibrium charge states were also determined. The latter agree with the values given in the literature [6].

Quantitative depth profiles

Absolute elemental contents can only be determined when the number of projectiles is measured and the charge state distribution of the detected element is known. In order to overcome problems with the correct measurement of these parameters a monitor counter was installed in the scattering chamber of the Q3D for simple ERD-measurements with a good Z-resolution for all light and medium heavy elements.

In order to achieve a quantitative depth profile not only an exact energy analysis but also the mean concentration of the elements to be investigated has to be determined. Therefore a ΔE-E_{res} telescope serves as a monitor detector in the target chamber and to identify the nuclear charge Z of the recoils. The mean value of the highly resolved depth profile is scaled by the stoichiometric ratio of the element observed. A new ΔE-E_{res} telescope, which consists of an ionisation chamber (ΔE measurement) and a pin-diode(E_{res}measurement) has been built (see figure 3) and replaced the old monitor counter consisting of a surface barrier detector and a pin diode.

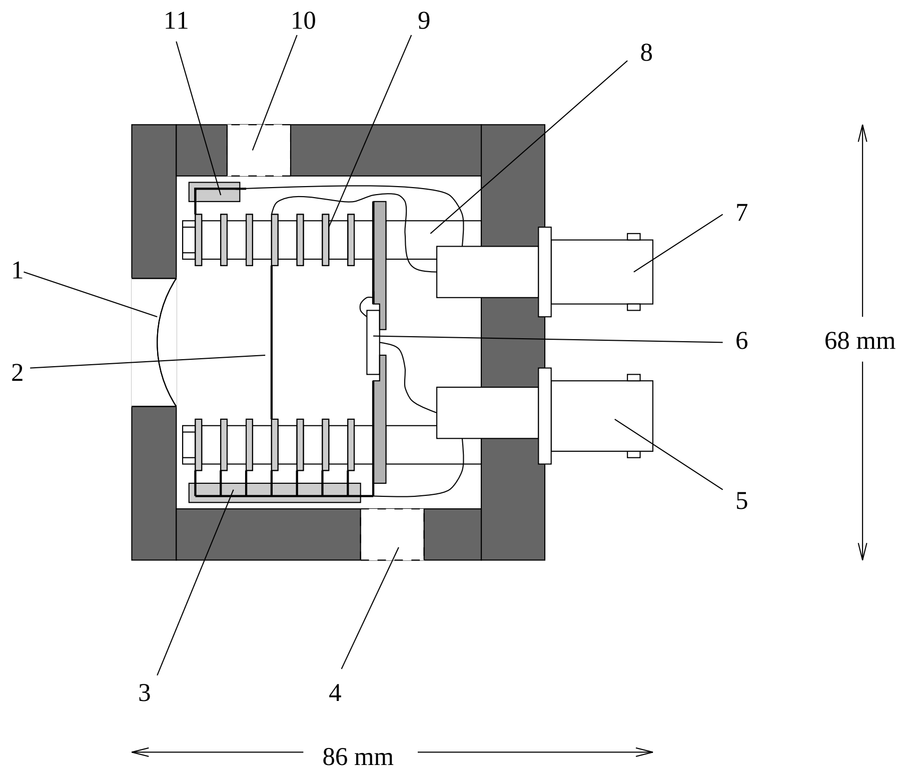

Fig. 3: Schematic diagram of the ΔE-E$_{res}$ telescope described in the text. The numbers correspond to: (1) entrance window, (2) anode, (3) resistor chain, (4) gas outlet, (5) BNC, (6) pin-diode, (7) BNC, (8) insulator spacers, (9) guard rings, (10) gas inlet, (11) resistor.

Advantages of the new monitor are:

- To achieve a good Z-resolution the energy loss in the ΔE detector should be about 50% [10]. As the gas pressure in the detector is variable from 0 up to 700 mbar the thickness of the ΔE detector can be varied according to the requirements of a wide range of specific experiments. Operating the ionisation chamber with a steady flow of an argon-methane mixture containing 90% argon and 10% methane (P10) elements from hydrogen to silicon could be seperated at a gas pressure of 300 mbar (figure 4 shows an example). Heavier ions should be separable with heavier ion beams and higher energies.
- Independent of the thickness, the homogeneity of a ΔE gas detector can be better than 1%.
- This type of telescope offers a compact construction combined with a broad dynamic range.
- As solid samples are being investigated, ions with velocities between just above zero and maximum velocity (recoils from the surface of the sample) enter the monitor counter. Due to the energy dependence of the Rutherford cross section many more slow ions leave the sample than fast ones. As a result far more ions are stopped in the ΔE counter than in the E$_{res}$ counter. Ionisation chambers are not subject to radiation damage. They are therefore more economic in operation as a ΔE counter and not subject to a degradation as we observed in the formerly used solid state ΔE-detector.

The electric field of the ionization chamber is parallel to the particle trajectory (axial chamber). The housing is made of stainless steel, grounded and connected with the aluminum coated mylar entrance window. With this type of chamber the field is homogeneous over the entire ionization volume. The

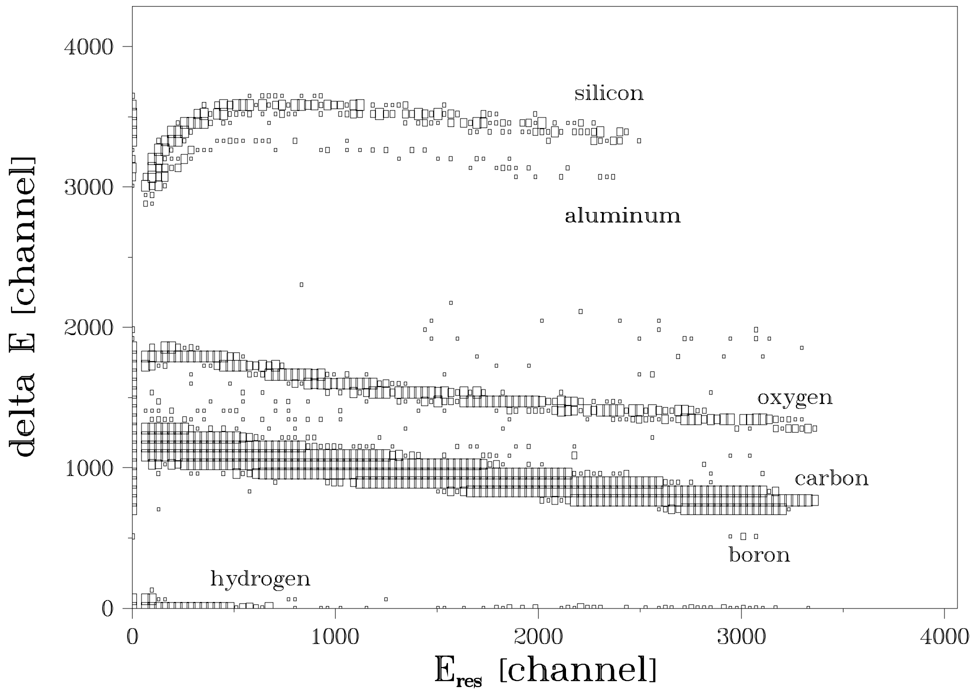

Fig. 4: A plot of energy loss in the gas (ΔE) versus energy deposited in the pin-diode (E_{res}), for a 130 MeV Ni ion beam on a diamond sample. The ΔE and E_{res} signals are triggered by the E_{res} signal and taken in coincidence. The number of counts with a particular value of ΔE and E_{res} is indicated by the size of the square at that point. The recoils having the largest atomic number suffer the largest energy loss in the gas, as indicated in the figure.

anode is situated half way between entrance window and pin-diode. So double the electric field strength in the active gas volume is obtained with the same voltage. This leads to high drift velocities and in this way to high possible counting rates without pile up. With maximum counting rates of 800 Hz until now no pile-up could be observed. The electron drift velocity is 12 cm/μsec in P10 with 400 Volts applied and at a gas pressure of 300 mbar [11]. So the counting rate is not limited by the electron drift velocity. The anode consists of a 35 μg/cm^2 aluminum foil. It is easy to handle and angle and energy straggling are no problem.

Sputtering with high energetic heavy ions

Measurements of the sputter yield of carbon were continued with several high energetic heavy ion beams [2]. The same multilayer samples as reported in [2] were used consisting of three thin layers of ^{13}C separated by ^{12}C layers deposited by thermal evaporation-condensation. The decrease of the surface ^{13}C content in comparison to the deeper layers with the ion dose gives the desired sputter yield. The sputter yield of carbon is enhanced by a factor 500 over that calculated with standard elastic scattering theory [9] when 120 MeV ^{197}Au ions [2] are used, while the sputtering induced by 60 MeV ^{127}I-ions is 200-times higher than calculated. In contrast no sputtering could be measured for 60 MeV ^{58}Ni ions because the sputter yield was lower than the deposition rate of hydrocarbons from the residual gas of the vacuum chamber which was about 2 carbon atoms per incident Ni-ion. In order to obtain also a value for carbon sputtering with Ni-ions, a better vacuum in the order of 10^{-7} Pa or better is required for a reliable sputter measurement not disturbed by adsorption processes.

This measurement gave us the hint that depth microscopy with 60 MeV Ni-ions should result in much lower irradiation damage effects than with the heavier ion beams. This would not be the case if pure elastic nuclear scattering would be responsible for the sputter process. Up to now it is not clear which process, obviously induced by the high electronic energy losses, produces the strong enhancement for the sputter yields. A decision whether coulomb explosion of the highly ionized target atoms in the ion channel leads to strong irradiation damage effects or a short high temperature thermal spike with high cooling rates after the passage of the ion makes the effects (both discussed in literature, see for example [13] and [12]), eventually can be given when systematic sputtering investigations are performed with different types of carbon.

Mixing zones of carbon films deposited with laser plasma ablation-condensation
(in cooperation with Ch.M. Frey)

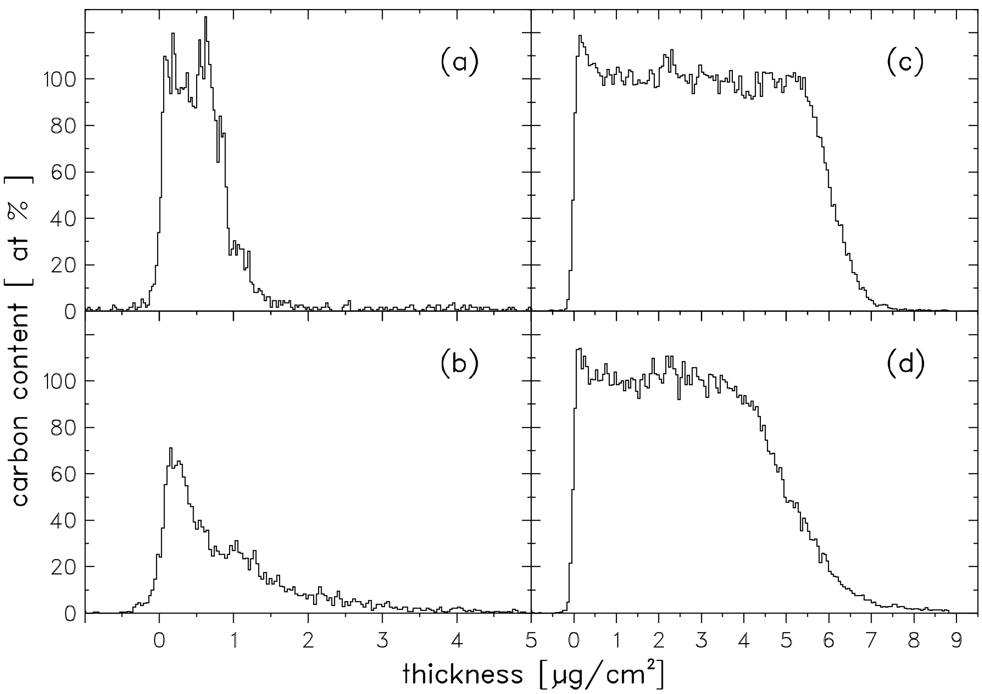

Fig. 5: Carbon profiles ($^{12}C^{5+}$ analysed) of carbon films deposited by laser plasma ablation-condensation with two different laser light intensities onto smooth crystalline silicon substrates. Two thicknesses were choosen for each type of carbon for the investigations of the mixing zone between the carbon films and the silicon. a), c) laser light intensity 2 GW/cm^2. b), d) laser light intensity 20GW/cm^2.

Carbon films deposited with different laser light intensities in the new plant for fabricating the new type of more ion beam resistant carbon stripper foils were investigated in order to obtain the mixing zones between the films and their substrates. Flat and smooth crystalline silicon substrates were used for these experiments. Fig. 5a shows the carbon profile of a film deposited with 20 GW/cm^2 laser light intensity. A long tail of the distribution of carbon can be recognized showing a large mixing zone. A thicker film (fig. 5b) shows a width of the mixing zone of 2.5 μg/cm^2 between 13% and 87% carbon content. In contrast to that a carbon film deposited with 2 GW/cm^2 shows a much thinner mixing zone (figs. 5c and 5d) of 0.6 μg/cm^2. In these spectra the larger width of the slope at the interlayer of the thicker film with the substrate (fig. 5d) is due to a worse depth resolution at this depth. But a depth resolution of 0.1 μg/cm^2 can be seen at the surface of the thin carbon film [14]. The investigations showed that the large mixing zones can be responsible for a strong adhesion of the films on the substrates. Therefore thicker parting agents or a protection layer of carbon deposited by thermal evaporation-condensation, producing no mixing zone, should be used in order to get an efficient foil production.

[1] *Jahresbericht des Beschleunigerlabors 1990.*
[2] *Jahresbericht des Beschleunigerlabors 1991.*
[3] G. Dollinger, T. Faestermann, P. Maier-Komor: *Nuc. Instr. and Meth. B64 (1992) 422.*
[4] G. Dollinger: *12 th Int. Conf. on the Appl. of Accelerators in Research and Industry*, Denton, 1992, to be publ. in Nucl. Instr. and Meth. B.
[5] G. Dollinger, M. Boulouednine,T. Faestermann, P. Maier-Komor, H.-J. Körner: *to be publ. in Rad. Eff. Def. Sol.*.
[6] M. Boulouednine: *diploma theses*, Technical University of Munich, 1992.
[7] W. Mayer: *thesis*,Technical University of Munich, 1985.
[8] M. Löffler, H.-J. Scheerer and H. Vonach, Nucl. Instr. and Meth. 111 (1973) 1.
[9] J.F. Ziegler, J.P. Biersack and U. Littmark: *The Stopping and Range of Ions in Solids*, Pergamon Press, New York, vol. 1 (1985).
[10] K. Bethge,R. Martin,H. Stelzer: *Experimental Methods in Heavy Ion Physics*, Springerverlag (1978) S.178.
[11] S. Flügge: *Handbuch der Physik*, Springerverlag 45 (1958).
[12] C. Dufour et al.: *MRS-conf*, Straβbourg, Nov. 1991.
[13] R.L. Fleischer, P.B. Price and R.M. Walker: *Nuclear tracks in solids*, University of California Press, 1975.
[14] G. Dollinger, M. Boulouednine, T. Faestermann and P. Maier-Komor: *16 th World conf. on INTDS*, Nucl. Instr. and Meth. A, to be publ..

2.5.3 Materials Analysis with Heavy Ion Beams

W. Assmann, W. Hering, H. Huber, S. Ißmer, T. Michalka, P. Staat, A. Weidinger, Th. Winkelmann, E. Wolf

A dedicated beamline for materials analysis was installed this year. It consists of two vacuum chambers, one for RBS (Rutherford backscattering spectroscopy) and one for ERDA (elastic recoil detection analysis). The ERDA chamber is equipped with a computer controlled sample positioning system and a position sensitive gas ionization counter. This new setup was used for analysis of samples from different fields of application ranging from high-T_c superconductors and fusion reactor materials to targets for nuclear physics. In addition a small UHV chamber was built for measurements of sputter yields from high energetic heavy ion bombardement. With this setup first experiments were done on various metals using the catcher technique for detection of sputtered particles.

New installations for materials analysis

In the last 3 years ERDA measurements were done with the experimental setup for subcoulomb transfer reactions [1]. The use of an existing setup and the experience of Th. Winkelmann was a great help in coming up so quickly with ERDA measurements. With this background a new beamline was designed and installed in target hall II at 50° beam deflection dedicated for RBS and ERD analysis. The general layout of the beamline is shown in fig. 1:

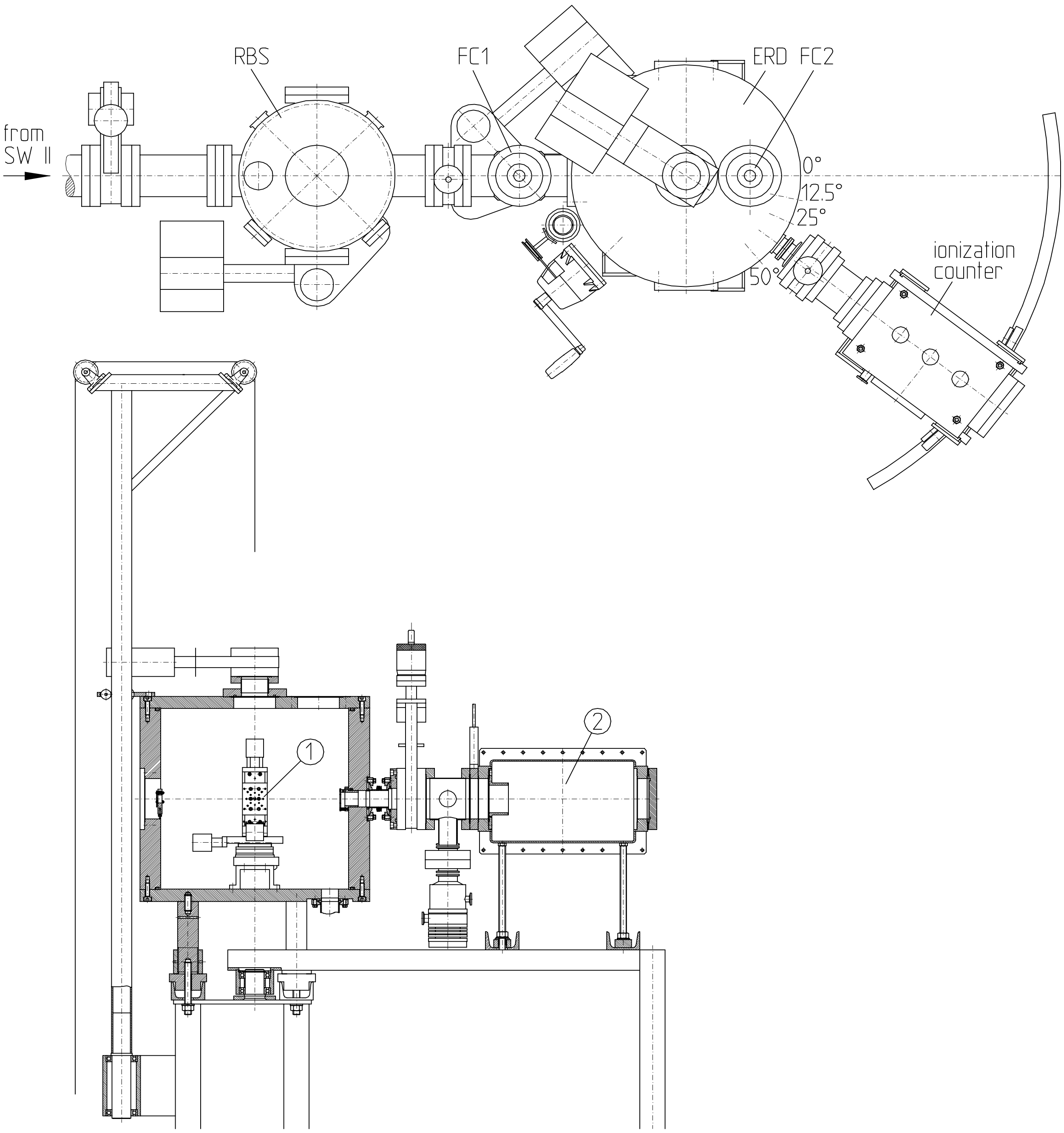

Fig. 1: General layout of the beam line for materials analysis. The first chamber is mainly for RBS (Rutherford backscattering spectroscopy), the second chamber for ERD (elastic recoil detection) analysis. The recoils are detected by the ionization chamber which can be connected to the vacuum chamber at 5 different angles. FC1 and FC2 are Faraday cups. The beam comes from switching magnet II (SW II) at $+50^o$. At the lower part of the figure a side view of the ERD chamber is shown: 1 indicates the goniometer, 2 the ionization chamber

The main components are a vacuum chamber for RBS, a first faraday cup, the vacuum chamber for ERDA including a second faraday cup, and the gas ionization counter, which can be connected to the vacuum chamber at five different scattering angles.

The RBS chamber contains a mounting platform for semiconductor counters (SBD or PIN diodes) at different scattering angles and distances. The sample handling system consisits of two rotatable target wheels, a first one with 9 positions for ERDA in transmission geometry, a second one for RBS with 18 positions. The beam position on the sample can be controlled with a TV camera. The vacuum in the RBS chamber during measurements is in the 10^{-7} Torr range. Data recording is done by an ATARI based multichannel analyzer (OIMEL) using the GP-interface [2].

The ERDA vacuum chamber (fig. 1) has 45 cm inner diameter and 45 cm height to house a sample positioning system including the stepper motors [3]. The system allows linear sample movements in all three dimensions and a rotation around an axis perpendicular to the scattering plane. With this goniometer construction, the incidence angle of the beam onto the sample surface can be changed without moving the beam spot on the sample. For remote control of the system, the ATARI computer with the GP-interface mentioned above is used. Although the goniometer components were originally not designed for use in vacuum, it was possible to reach a base pressure in the chamber of 10^{-7} Torr with only minor changes of the goniometer (Teflon cables, uneloxated Al-surfaces). Sample holders with up to 12 sample positions can be exchanged very quickly using a load lock system.

The recoils in ERDA measurements are detected with a newly built ΔE-E_{rest} gas ionization counter of essentially the design of U. Quade. The cathode has a backgammon structure which allows a position sensitive detection of the particles. With this arrangement, a Z-identification of the recoils and a simultaneous correction of the kinematic shift is possible. The latter is necessary since the large acceptance angle of the detector of about 10 msr would destroy the energy resolution. This detector therefore combines high detection efficiency (i.e. low radiation damage) with good energy (i.e. depth) resolution.

Fig. 2 shows as an example a 2-parameter plot of ΔE and E_{rest} for Z-identification and a plot of the X-Y coordinates in the chamber for position determination. Both measurements were performed on a thin layer of TiON on Cu coated glass (Prof. Sizmann, LMU); for the X-Y measurement a calibration mask with vertical and horizontal holes was put in front of the detector. The angular resolution is about 0.05 degrees, with the kinematic correction a depth resolution of better than 10 nm can be achieved.

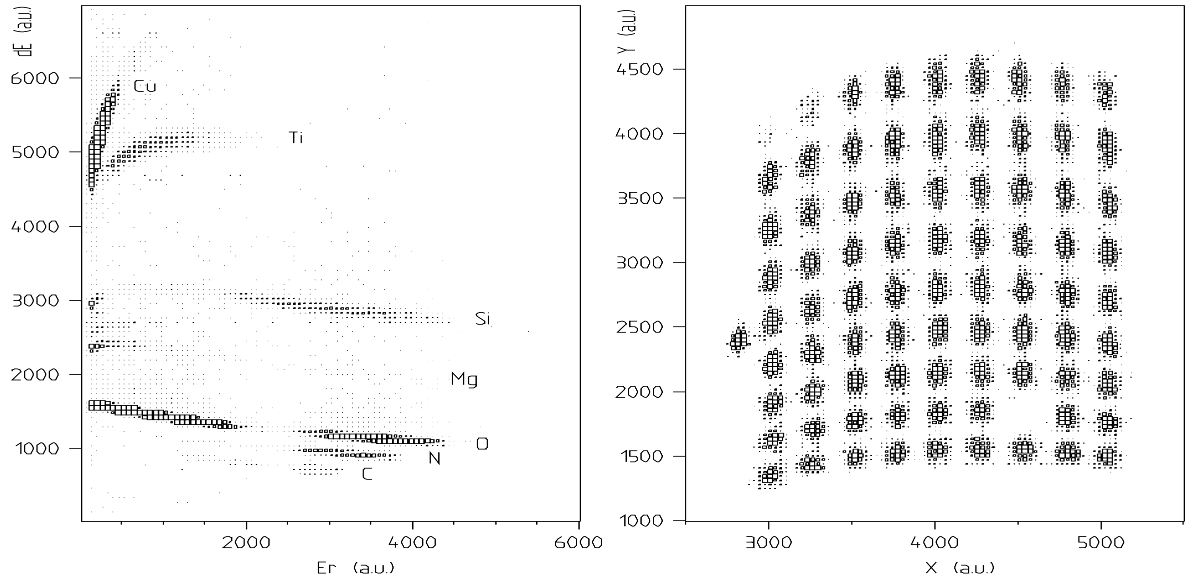

Fig. 2: Example of an ERD analysis of a TiON film on Cu coated glass. (left side) ΔE and E_{rest}-matrix measured with the ionization chamber, different elements are indicated. (right side) X-Y matrix of the particle position in the ionization chamber. A mask with 6 mm separated holes in X and 4 mm separated in Y was put in front of the chamber, the hole diameter is 2mm.

First test experiments for the sputtering program with ^{127}I beams showed that UHV conditions are necessary in order to avoid interference with surface contaminations [5]. Therefore a small UHV setup was built to improve the vacuum conditions in further experiments [6]. The main components are a 230 l/s turbomolecular pump and a Ti sublimation pump with LN_2 baffle, a quadrupole mass spectrometer, a cold cathode UHV vacuum gauge, and a saddle field sputter gun for surface cleaning. As a first application of this setup the UHV compatibility of a large 6cm x 6cm carbon foil fixed with a carbon emulsion on a metal frame was shown. Such a test was required prior to the installation of the foil in the ESR vacuum at GSI. After 48 hours backout of the whole setup at around 220^o C, a pressure of 1*10^{-11} Torr was reached with that foil built in. A second UHV test of an ESR component (PIN diode array) with this setup is described elsewhere in this report.

RBS and ERD analysis with heavy ions

25 MeV ^{16}O beams were routinely used to measure the stoichiometry of high-T_c superconductor films epitaxially grown by thermal co-evaporation on different substrates (Prof. Kinder, TUM). A special question was the homogeneity of YBCO films on large area substrates, e.g. 3" diameter wafers, investigated with this method. It could be shown with our RBS analysis, that the stoichiometry across the wafer is constant within about 2%.

The standard beam for ERDA measurements was ^{127}I with 140 to 170 MeV energies, the ionization counter was mounted at an scattering angle of 37.5^o to prevent elastic beam scattering into the detector for most of the sample components.

We continued our investigation of impurities in targets for nuclear physics experiments (H.J. Maier, LMU) using the ERDA technique in transmission geometry and PIN diodes in case of light element contaminations and the ionization chamber with Z-identification for heavier impurities. The origin of two target impurities mentioned in the last annual report [7] is now clear: the Si contamination found in almost all targets at a concentration level of about 10^{-4} at% could be traced to the parting agent betaine. The high C content in some sputter deposited targets, especially in Mo targets, seems to be connected with the carbon support plate of the sputter pellet.

A further experiment was concerned with the depth distribution of the implanted light elements in the wall probes from the reactor vessel after the first (d,t)-fusion in the tokamak experiment JET (Culham, England). We performed measurements on inner-wall sample materials with the new ERDA setup. In addition to the ionization counter, a surface barrier detector telescope with an absorber foil was installed to look for p,d, and t recoils. The particle separation was adequate for these three isotopes, but the sensitivity for the expected small t concentrations was to low. This experiment was carried out in cooperation with R. Behrisch (IPP Garching), and R. Grötzschel and U. Kreissig (FZ Rossendorf) who helped us also in the last phase of the beam line installation.

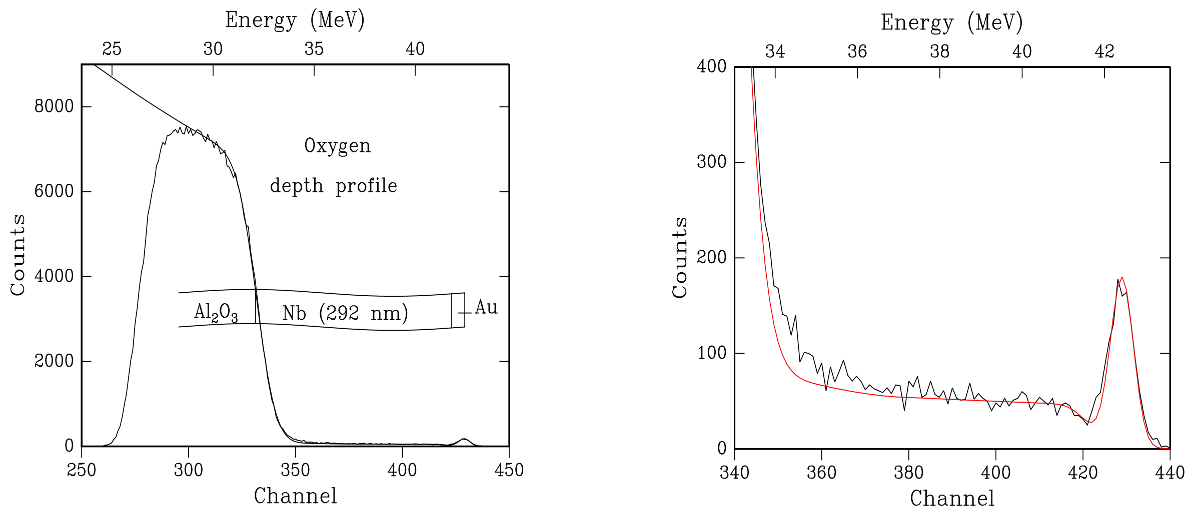

Fig. 3: Oxygen depth profile of an Au(15nm)/Nb(292nm) film on saphire substrate. The right figure shows an expanded view of the high energy part. The smooth line is a simulation of the data assuming a constant O concentration of O/Nb=1.5 at% in Nb and no O-content in Au. An additional O peak from surface contamination is seen.

The ERDA technique is well suited to measure the oxygen concentration in thin films with high precision. First experiments were done on YBCO films (Prof. Kinder, TUM and Prof. Stritzker, Uni Augsburg) and on Nb and NbTi samples (A. Weidinger, HMI Berlin). As an example the oxygen concentration in an epitaxial Nb film on a saphire (Al_2O_3) substrate is shown in fig. 3. The film was covered with a Au layer in order to prevent the oxidation on air. Also shown in the figure is a simulation of the data with the RUMP program; the normalisation was derived from an adjustment of the fit to the substrate. The analysis yields an oxygen concentration in the Nb film of [O]/[Nb]= 1.5 at%.

Sputtering with high energetic heavy ions

Radiation damage and sputtering can become important and therefore has to be considered in materials analysis with HI; so far only very few measurements are published in the relevant energy range of 1-2 MeV/u. This field is also interesting in itself since new (electronic) mechanisms for the energy loss above 10 keV/nm could possibly enhance the sputter yields. On the other side sputter measurements with tandem beams are difficult because of low beam currents available for HI. Thus one has to apply sensitive measuring techniques.

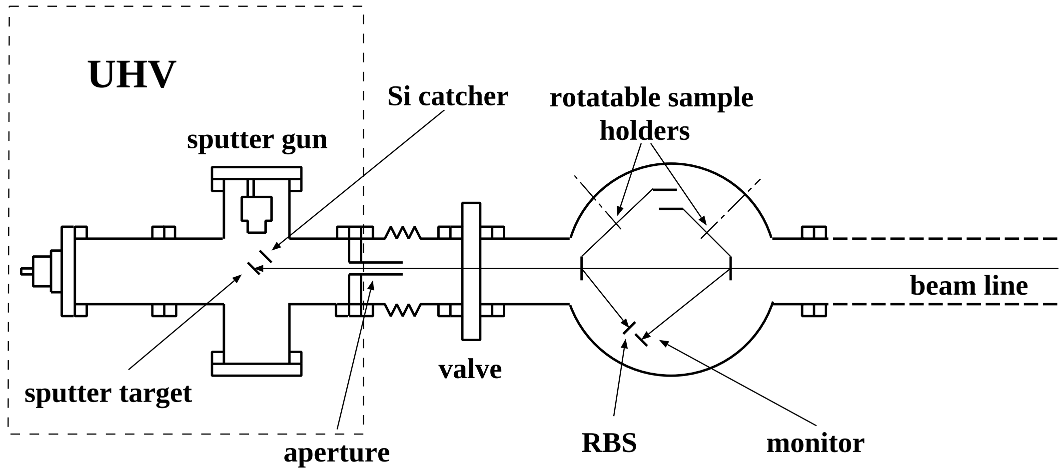

Fig. 4: Experimental setup for the sputtering experiments. The sputter geometry, the beam monitoring system and the RBS analysis position can be seen.

One possibility is the catcher technique, where the sputtered particles are collected on a catcher foil and afterwards detected by RBS. First test measurements with 60 and 140 MeV ^{127}I ions [5] at a pressure of 10^{-6} Torr showed enhanced sputter yields compared to simulations with the computer code TRIM.CASCADE (J.P. Biersack). However, due to the undefined surface conditions, i.e. oxydation and adsorbates, quantitative measurements were impossible. To ensure well defined surfaces on the sputter targets the UHV setup was used for further measurements separated from the beam line through a small aperture for differential pumping (fig. 4).

Si catcher and sputter target were backed for 2 days at 200° C together with the whole UHV system. With the valve to the beam line open a basic pressure of $3{*}10^{-9}$ Torr could be reached in the UHV chamber. Before the sputter measurement started, the sputter target surface was cleaned with 8 KeV Ar ions (30 μA, 30 min). The Si catcher was protected from sputtered particles during this time by a removable shutter. The sputter cleaning procedure was repeated after half of the measuring time.

Two measurements of the sputter yield with a 140 MeV ^{127}I beam on a Cu target were made, one with and one without sputter cleaning of the target, resulting in an enhancement factor of 5 and 26 compared to TRIM simulations, respectively. At present, the data are not conclusive because of i) large statistical errors (only about 1 atomic monolayer was sputtered off within 3 hours) and ii) insufficient vacuum conditions which can influence sputter yields drastically.

For further sputter measurements the vacuum conditions and the detection method will be improved: The UHV chamber will be separated from the beam line vacuum by an additional pumping stage and the sputter effect will be measured by the ERDA method. In this way the sputter yield can be directly derived from the decreasing counting rate of particles from the surface layer [8]. Fig. 5 shows the result of a first experiment with 140 MeV ^{127}I ions on a Al/Cu multilayer target at nearly glancing incidence of 3^o. In the recoil energy spectrum, the Al and Cu layers can be clearly separated, the depth resolution for the Al surface layer is better than 10 nm.

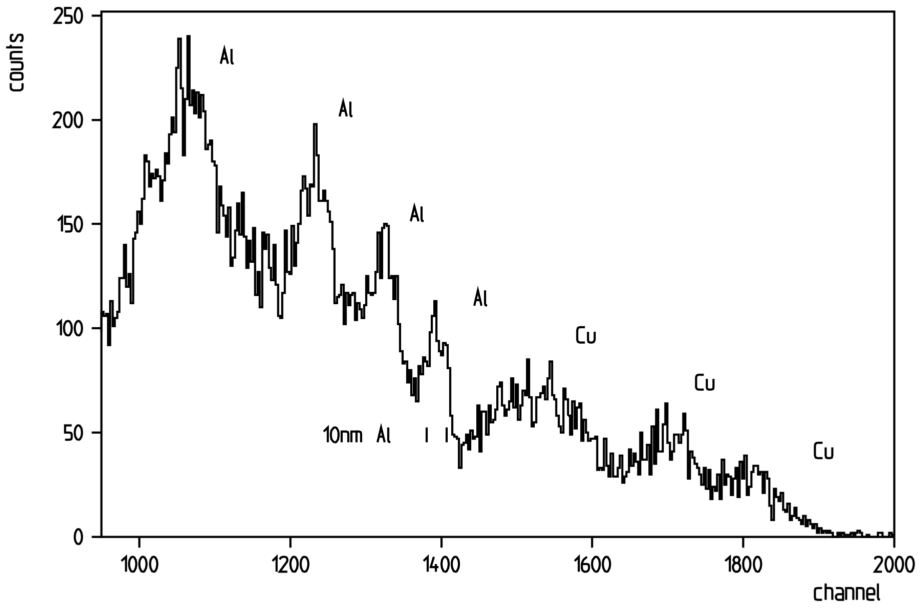

Fig. 5: Recoil energy spectrum of a Al/Cu multilayer measured with a PIN diode in ERDA geometry, and 140 MeV ^{127}I ions at an incidence angle of 3°. The right two Al peaks correspond to 10 nm thickness each and are separated by a 5 nm Cu layer.

[1] Jahresbericht 1990, p.185
[2] G/P electronics, Berlin
[3] OWIS, Staufen i. Br.
[4] P. Staat, diploma thesis, LMU München 1992
[5] E. Wolf, diploma thesis, LMU München 1992
[6] S. Ißmer, diploma thesis, LMU München 1992
[7] Jahresbericht 1991, p.94 and 141
[8] Jahresbericht 1991, p.98